Signature: © Pol J Radiol, 2010; 75(3): 25-37

Polish Journal of Radiology
www.PolRadiol.com

REVIEW ARTICLE

Received: 2009.04.29
Accepted: 2009.06.15

Salivary gland calculi – contemporary methods of imaging

Iwona Rzymska-Grala[1], Zygmunt Stopa[2], Bartłomiej Grala[3], Marek Gołębiowski[1], Hubert Wanyura[2], Anna Zuchowska[1], Monika Sawicka[1], Michał Zmorzyński[2]

[1] I Institute of Clinical Radiology of the Medical University of Warsaw, Warsaw, Poland
[2] Cranium, Jaw & Face Surgery Clinic of the Medical University of Warsaw, Warsaw, Poland
[3] Department of Pathology of the Military Institute of Medicine, Warsaw. Poland

Author's address: Iwona Rzymska-Grala, I Institute of Clinical Radiology of the Medical University of Warsaw, Chałubińskiego 5 Str., 02-004 Warsaw, Poland, e-mail: irzymska@esculap.pl

Summary

Sialolithiasis is the most common disorder of major salivary glands. The main site of salivary stones' formation is submandibular gland, followed by parotid and sublingual gland. The aim of this article was to present current diagnostic imaging modalities carried out in patients suspected with salivary stones on the basis of own material and review of literature.

Current diagnostic imaging tools used in the imaging of salivary stones were described and illustrated in this paper. These are: conventional radiography, sialography, ultrasonography, computed tomography, magnetic resonance sialography and sialoendoscopy.

Digital subtraction sialography and ultrasonography are the methods of choice in the imaging of salivary gland calculi. Although sialography is a very old diagnostic method, still it is the best diagnostic tool in the imaging of subtle anatomy of salivary gland duct system. Digital subtraction sialography can show the exact location of salivary stone and enables imaging of salivary ducts' pathology (e.g. stenoses), which is especially important when sialoendoscopy is planned. Sialography is also used as the treatment method, i.e. interventional sialography. Nonenhanced computed tomography is recommended when multiple and tiny salivary stones are suspected. Magnetic resonance imaging is the evolving alternative diagnostic method. In this diagnostic modality there is no need for salivary ducts' cannulation and administration of contrast material. Thus magnetic resonance sialography can also be carried out in the acute sialoadenitis. In the future, sialoendoscopy may become one of the main diagnostic and treatment procedures for salivary duct disorders, especially in salivary stone cases.

Key words: **sialolithiasis • salivary gland calculi • salivary stones • sialography • diagnostic imaging**

PDF file: http://www.polradiol.com/fulltxt.php?ICID=881145

Background

Sialolithiasis is the most common disorder of major salivary glands [1]. One of the post-mortem studies revealed calculi in the salivary glands in 1.2% of the population [2]. The most symptomatic sialolithiasis can be observed in patients between 30 and 60 years old [2]. According to one of the etiopathogenetic theories, the formation of the salivary gland calculi results from a deposition of calcium salts around a core made of desquamated epithelial cells, foreign bodies, bacteria, or mucus. Salivary gland calculi are of laminal structure (Figures 1–3). Their main inorganic component are phosphates and calcium carbonates [3]. The stones may reach from 0.1 to 30 mm (Figure 4) [2]. In one of their papers, Drage et al. [2] quoted a mean size of the parotid and submandibular stones of up to 3.4 mm (range from 1.5 to 9 mm), and a mean number of stones per one patient, 1.67 (range from 1 to 5).

The most common site of calculi formation is the submandibular salivary gland – 80% (60–90%). Approximately 10–20% (5–20%) of stones are located in the parotid gland,

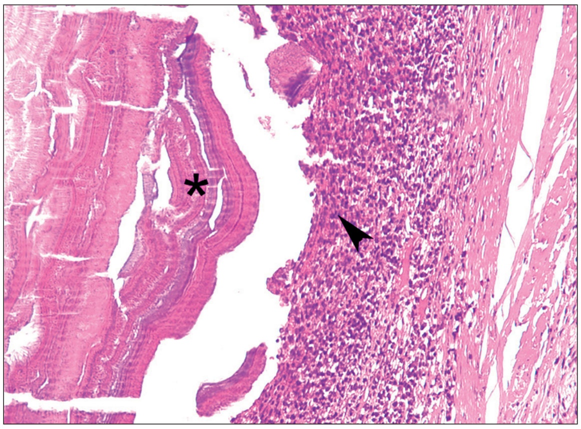

Figure 1. Large calcified stone inside the excretory duct of the submandibular salivary gland (*). Laminar structure of the stone is clearly visible. The stone caused ulceration of the duct's wall (arrowhead). (Histological material from the collection of Pathomorphology Institute of the Medical University of Warsaw).

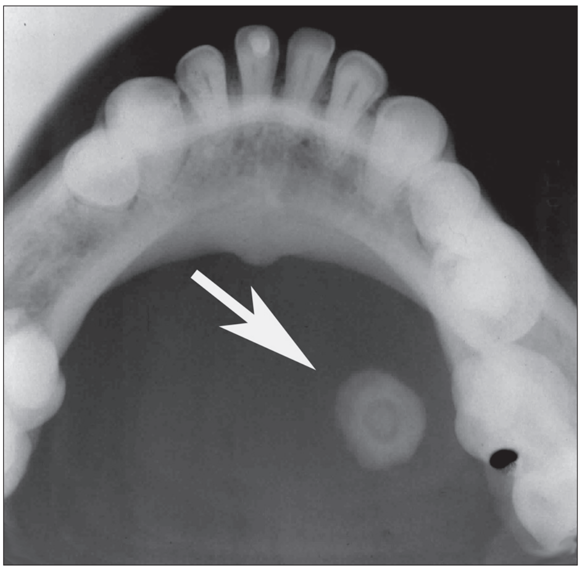

Figure 2. Mandibular occlusal view, the arrow points a large calcified stone (9×8 mm) in the left Wharton's duct. The laminar structure of the stone can be seen. (own material)

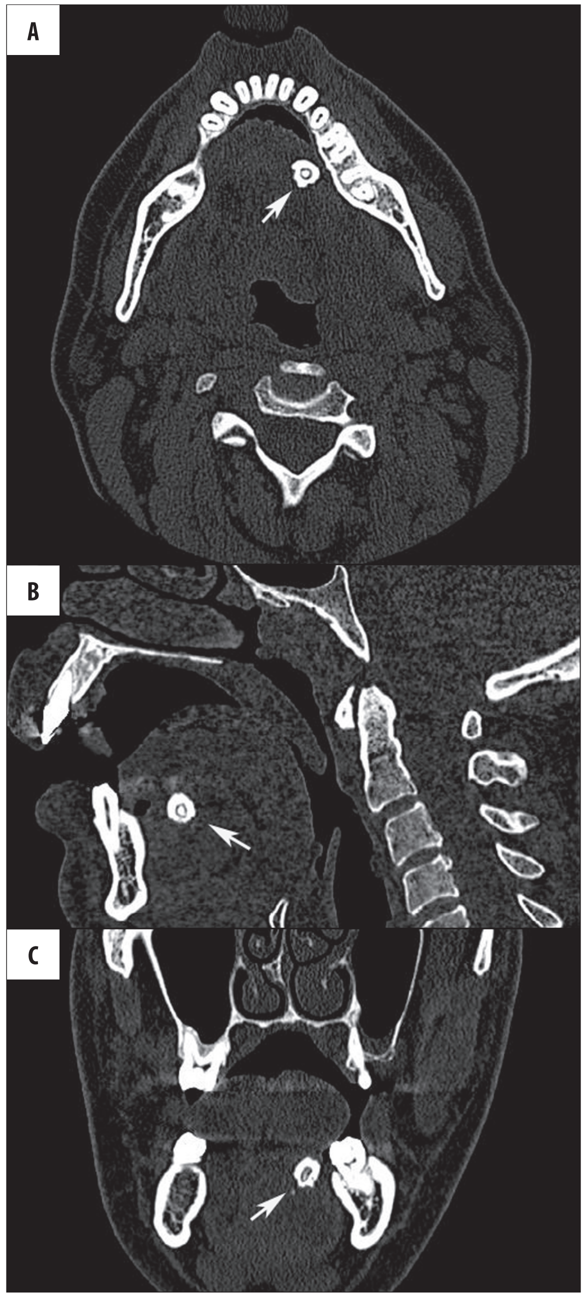

Figure 3. Nonenhanced computed tomography (CT). (**A**) – axial bone CT, large, round, calcified stone (8×8 mm) in distal segment of the left Wharton's duct (arrow), (**B**) – the same calcified stone (9×8 mm) in sagittal view, (**C**) – the same stone (9×8 mm) in coronal view. The laminar structure of the stone can be seen (courtesy of Czasopismo Stomatologiczne)

and 1–5% in the sublingual gland [1,2,4-9]. In 25% of cases, the stones are multiple [1,4,5,8].

Submandibular gland is the most common place for calculi formation because it produces a particularly viscous, mucous and more alkaline saliva, with a relatively high concentration of hydroxyapatites and phosphates. This predisposes to the precipitation of salts [1,5]. Moreover, the opening of the main salivary duct of the submandibular gland (Wharton's duct) is narrower than the diameter of the whole duct. What is more, the duct ascends towards its opening, which is also conducive to saliva retention [3,5,8,10].

As much as 85% of submandibular gland stones are located in Wharton's duct, while the remaining 15% in gland parenchyma [8]. Calculi situated in glandular parenchyma do not tend to cause significant clinical symptoms [5,11].

It is rare for a large stone located in Wharton's duct not to produce any symptoms of inflammation or pain [5]. The most common site of Wharton's duct for calculi formation is its proximal segment, in which the duct wraps around the posterior edge of the mylohyoid muscle, at a steep angle. That is where 35% of the deposits are located. Thirty per cent of the calculi are located near the opening of the submandibular duct, and 20% in its medial part [1,8,12]. Sjögren's syndrome and sarcoidosis promote calculi formation [5].

Figure 4. Spontaneously excreted salivary stone from the left Wharton's duct. Uneven surface of this calculus (10 mm) can be seen.

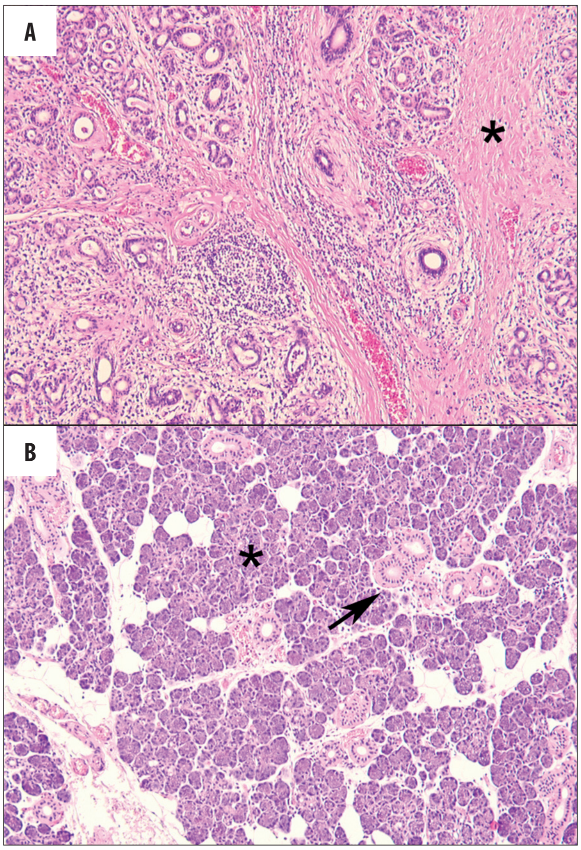

Figure 5. (**A**) Figure presents the submandibular gland with chronic sclerosing sialoadenitis, the main cause of which is sialolithiasis. Secretory units are destroyed by chronic inflammation. Excretory ductules became dilated. Massive collagenisation around them and between lobules is evident (*). (**B**) –The structure of normal submandibular salivary gland. Arrow indicates clustered fine excretory ductules, (*) – secretory units. (Histological material from the collection of Department of Pathology of the Military Institute of Medicine in Warsaw).

Symptoms of sialolithiasis do not differ much from the symptoms of other salivary duct obstruction causes. They include: a transient, painful, postprandial oedema of the salivary gland, gradually retreating in 2–3 hours, and pain during meals. A decreased production of the saliva may be observed as well [1,5,7,9,13].

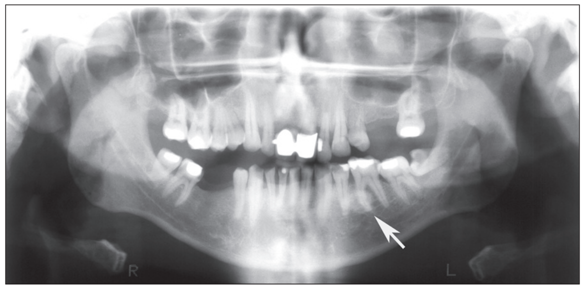

Figure 6. Pantomograph, calculus in the distal segment of the left Wharton's duct (arrow) (own material).

Sialolithiasis is the cause of 42–77% of cases of salivary duct obstruction [14,15]. Recurrent and chronic obstruction leads to saliva retention, infection and inflammation, being the cause of the chronic salivary gland oedema [1,16].

Sialolithiasis is concerned the most frequent cause of acute and chronic sialoadenitis [2]. Moreover, complications of sialolithiasis include: secondary infections, abscess, salivary duct stenoses, mucocele, Kuttner's tumour and glandular parenchyma atrophy in chronic states [1,8]. It is worth noticing that the Kuttner's tumour is a pseudo-tumour of the submandibular gland, with calcifications. It results from a chronic, sclerosing inflammation of that gland (Figure 5), due to lithiasis or autoimmunological diseases. Sometimes it is idiopathic. The submandibular gland is then hard and enlarged, and the physical examination is suggestive of a neoplastic lesion. Kuttner's tumour is connected with a characteristic inflammatory salivary duct distension. According to some authors, a diagnostic examination that may be decisive in such situations is the FNAB of the salivary gland with an ongoing pathological process [1,5].

Basic imaging methods of sialolithiasis are: X-ray images, X-ray sialography, ultrasonography (US), computed tomography (CT), magnetic resonance imaging (MRI). Sialoendoscopy, which is also a therapeutic method, is becoming increasingly common.

In the USA, a major role in sialolithiasis diagnostics is played by unenhanced computed tomography, while in Europe this is ultrasonography and digital subtraction sialography [1]. MRI sialography is also gaining on popularity.

X-ray Images

Intraoral (Figure 2) and extraoral (Figure 6), i.e. orthopantomogram, X-ray images allow for opaque calculi visualisation [6,11,17].

Approximately 80–90% of the stones are opaque on a standard review X-ray. However, up to 20% of the calculi cannot be revealed with a review X-ray [1,7,8,10].

It was observed that the stones of the submandibular gland produce opacity only in 80–90% of the cases, while the

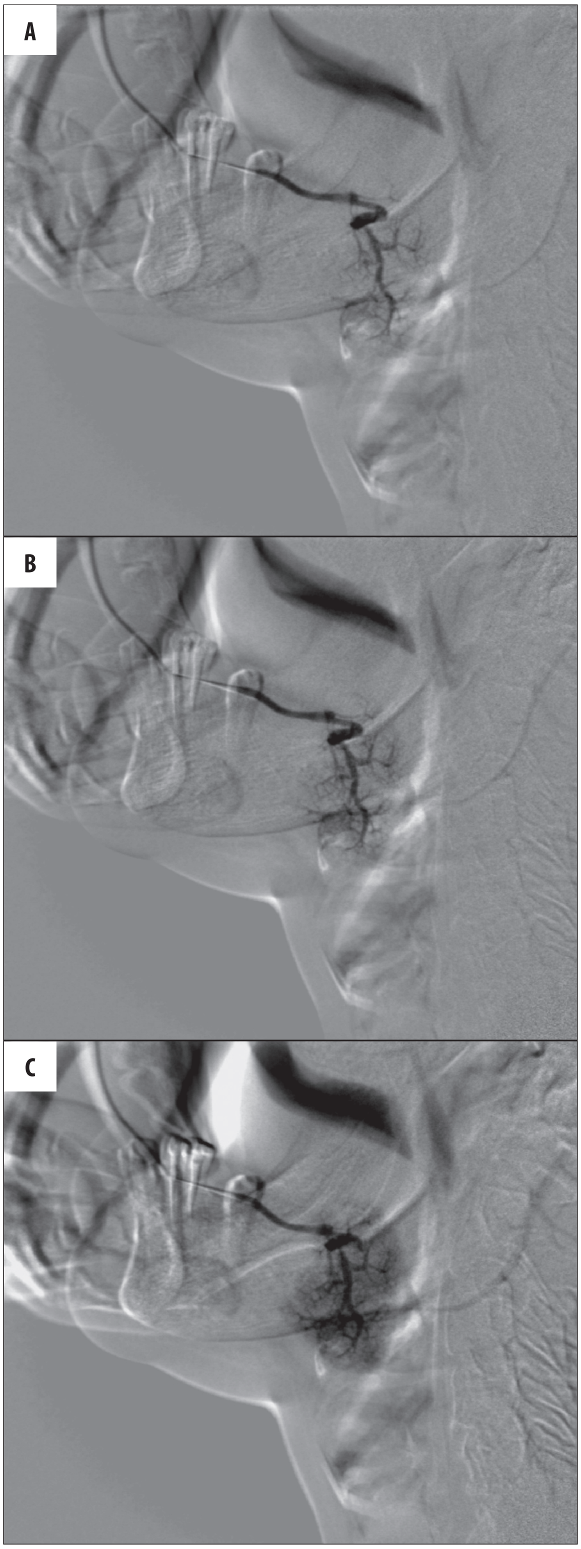

Figure 7. Normal submandibular digital subtraction sialography, lateral projection; (**A**) – the ductal phase, the Wharton's duct and the main intraglandular branches can be seen, (**B**) – the filling of the tertiary intraglandular branches can be seen, (**C**) – parenchymal phase (courtesy of Czasopismo Stomatologiczne)

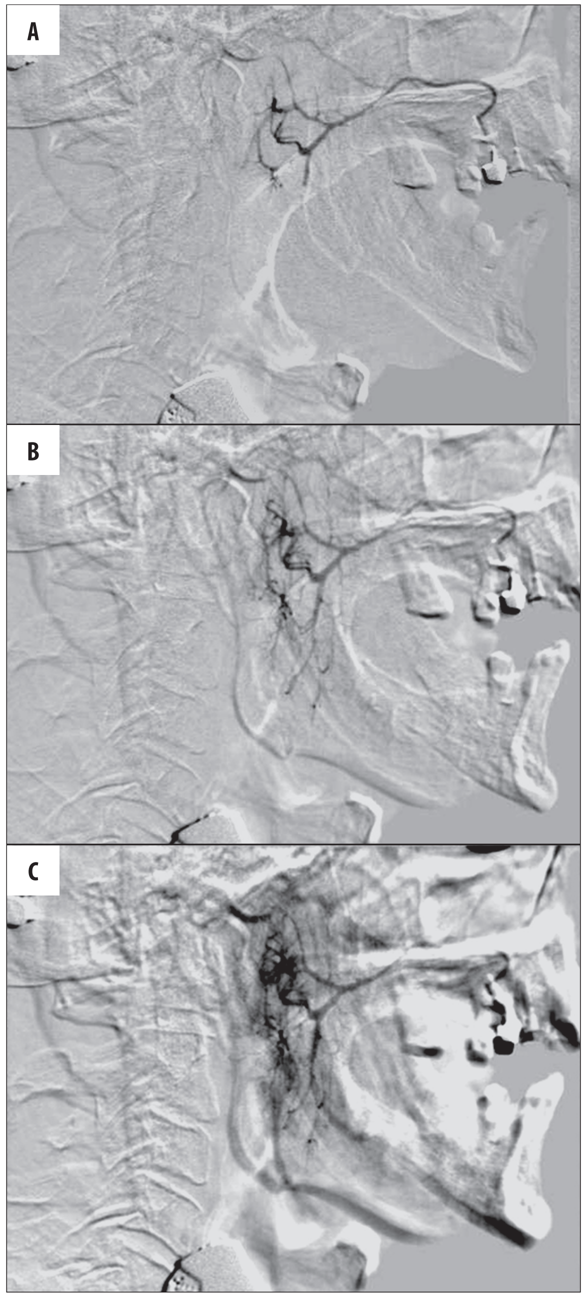

Figure 8. Normal parotid digital subtraction sialography, lateral projection; (**A**) – the ductal phase, the Stensen's duct and the main intraglandular branches can be seen, (**B**) – the filling of the tertiary intraglandular branches can be seen, (**C**) – parenchymal phase (courtesy of Czasopismo Stomatologiczne)

stones of the parotid gland only in 60%. Sialolithiasis of the sublingual gland is very rare [1,4,6].

A single X-ray normally preceds by sialography before contrast administration.

Sialography

Sialography visualises the ducts and the parenchyma of the salivary gland, after contrast administration into the main

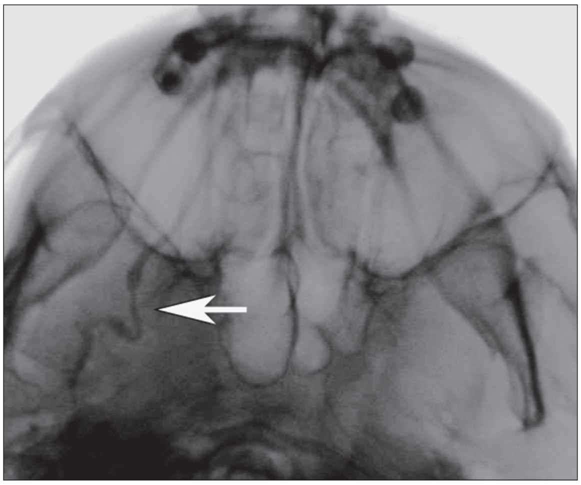

Figure 9. Conventional sialography of the right submandibular gland (axial projection), the stenotic segment of the right Wharton's duct can be seen (arrow) (courtesy of Czasopismo Stomatologiczne)

salivary duct. For decades it has been the main diagnostic method in the salivary glands [18]. The beginnings of the sialographic studies are dated 1902 [17].

Initially, bismuth was used to fill the excretory salivary ducts. In 1925, Carlsten introduced Lipiodol to sialographic studies, which was then replaced with Ethiodol, due to single cases of induction of granulomatous reactions. From time to time, when trying to obtain a better saturation of the salivary gland parenchyma (parenchymogram), the clinicians used a iodine solution as a contrast medium – Renographine [18].

Currently, a standard procedure uses water-soluble non-ionic iodine contrast media. There are those who still prefer to use oily contrast media (e.g. Lipiodol) which, in comparison to water-soluble preparations, remain in salivary ducts longer and produce more distinct sialographic images [19]. However, the escape of the oily contrast medium outside the salivary ducts may cause fibrosis of the glandular parenchyma [20].

During sialography of a normal, unaffected by any pathological process salivary gland, the administered contrast medium fills the peripheral parts of salivary ducts backwards, up to the gland. The image resembles tree branches, initially leafless, and gradually bursting into bloom. The 'bloom' of the tree, i.e. filling of salivary glands, is the moment of contrast medium introduction into the salivary gland parenchyma (Figures 7, 8) [17].

Sialography, and especially the digital subtraction sialography (DSS) is a recognised diagnostic method in suspicion of the salivary gland calculi, sialoadenitis, fistulas, as well as stenoses (Figure 9), and salivary gland dilatations, being helpful in their precise localization [9,16,18,19,21,22]. The examination visualises also non-opaque calculi in salivary ducts [4,6,11]. It is also excellent in revealing and localising calcifications close to salivary ducts [11]. This diagnostic tool allows for a high-certainty discrimination of the stone location: in the salivary duct or in parenchyma, which is crucial for the choice of a right therapeutic method [9].

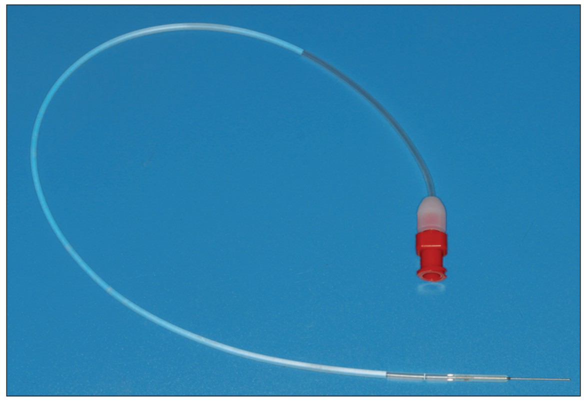

Figure 10. Rabinov sialography catheter.

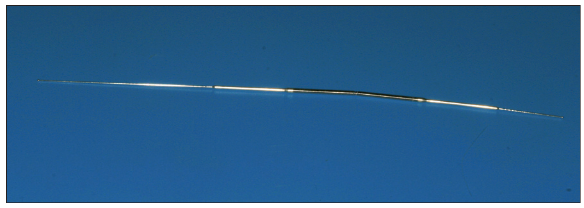

Figure 11. Salivary duct dilator.

However, this in not a method of choice in salivary gland tumour diagnosis [16,23–25]. Nowadays, sialography and its modified version, CT sialography, are largely replaced with CT and MRI in salivary gland tumour diagnostics. In suspicion of a malignant tumour, a recommended diagnostic tool is contrast-enhanced MRI [22].

Conventional sialography its static nature and presence of bony background [12,18]. The diagnostic reliability of sialography was improved after an introduction of digital subtraction sialography [26]. The use of post-processing enables for a subtraction of a bony background and contrast enhancement of the salivary ducts [12].

At present, sialography is performed rarely, and thus its methodics is worth revising.

During a sialographic examination, a patient remains in supine position. Most authors use Rabinov sialography catheters for this procedure (Figure 10) [11,22,27,28]. These are special catheters designed for cannulation of very thin salivary ducts. Different catheters are used for parotid (0.032 inch) and submandibular (0.016) salivary glands. Moreover, in order to carry out sialography, salivary duct dilators are needed (Figure 11), owing to which it is possible to dilate a salivary gland ostium, and to insert the Rabinov catheter into the salivary duct. In difficulties with salivary gland opening identification, or to facilitate catheter insertion, the patient may be given a small amount of the lemon juice, orally. This increases saliva production and exposes the excretory ducts [22].

Before the dilation and catheterisation of the salivary ducts, it is recommended to anaesthetise these regions locally with 10% Lidocaine in aerosol.

After catheter insertion, a water-soluble contrast medium is administered manually (usually by a radiologist) until patient's feeling of pain or substantial distention. This means that the contrast medium reached and filled the salivary gland parenchyma, which may be objectively observed during X-ray imaging as so called 'parenchymal blush' [12,18,19,26,29].

It is estimated that during sialography, in manual administration of the contrast medium, a mean injection rate amounts to approx. 0.01 ml/sec [19] – 0.1 ml/sec. [30] and a mean pressure does not exceed 75 mmHg (an approximate upper limit value of the excretory pressure in the salivary gland) [31]. The examination of the parotid gland involves the administration of approx. 1–1.5 ml of an aqueous contrast medium, while the examination of the submandibular gland: 0.5–1 ml [18]. Some authors describe a possibility of aqueous contrast medium administration with the use of the gravitational system, i.e. a drip placed about 70 cm above patient's oral cavity [32].

In sialographic examination, the images involve two projections, i.e. AP (or its modality, i.e. submentovertical vel axial projection) and lateral. The same kind of projections are used in parotid and submandibular glands [12,19]. Some authors report carrying out additional images, in oblique projections.

In digital subtraction sialography, every sequential study should be preceded by a control examination without contrast enhancement, so called mask. Before every change of projection, a decanniulation should be performed, to make sure that the contrast medium does not deposit in the ducts and falsify the results of the next series of images [12]. In the work by Buckenham et al. there were about 7–10 serial images taken in every projection – in the first 4 seconds with a frequency of 1/sec, and then at 1/2 sec. [12]. Due to the overlapping of the highest amount of bony structures, some of the authors used subtraction for lateral projections only [18,23]. A mean time of sialography amounts to 12–15 minutes [19,26]. Patients may feel a moderate tenderness and a slight oedema of the salivary gland for about subsequent 24 hours [2].

Some authors recommend late imaging, i.e. after 10 minutes from contrast administration, with or without an application of a sialogogue (e.g. lemon juice). Such imaging allows for a dynamic evaluation of contrast evacuation from the salivary ducts [32]. It is believed that late contrast medium emptying is characteristic for sialodochitis and sialoadenitis [33].

In one of their works, Hasson et al. used 22G catheters for contrast injection. The salivary duct opening was widened with the use of the salivary duct dilator. Next, 1.5–2 ml of a contrast medium was injected until the feeling of resistance. That is when the patient could feel distention and an increased pressure in this region. In order to avoid unpleasant sensations, the salivary ducts were anaesthetised from the inside, with the use of 0.5 ml Marcaine [13].

During sialography there are also interventional procedures undertaken under the control of X-ray television: interventional sialography. This is a less invasive method than the surgical treatment connected with a risk of nerve damage, postoperative infection, haematoma, and calculi formation. Yoshino et al. [34] removed successfully 63% of calculi with the use of fluoroscopy and the Dormia basket. Cases of treatment failure were connected with a strict fixation of a calculus to the wall of the salivary duct or inability to approach the stone with the use of a catheter, due to e.g. steep bend of the duct. The sizes of stones ranged from 2–9 mm, mean 4.3 mm. Return to a normal salivary function after intraoral removal of the stone was observed in 75% of the cases [34].

Indications for sialography include: suspicion of fine calculi, foreign bodies, stenoses, fistulas, diverticula, secondary lesions following an injury or infection. Sialography may also show: a communicating cyst, autoimmunological diseases and sialosis [33]. Contraindications for this procedure include an acute or chronic exacerbated sialoadenitis, iodine allergy and past adverse reactions to contrast media, planned isotopic examinations of the thyroid gland, pregnancy, possibility of a damage of the salivary duct opening, overfilling or tearing of the salivary ducts [6,19,35].

It is advised to wait approx. 6 week from the moment of inflammatory symptom relief, until sialography [19].

The disadvantages of sialography include: patient's exposition to ionising radiation and iodine contrast media; pain during contrast medium insertion into the salivary ducts; possibility of calculi dislocation towards the inside of the gland; quality of examination results depending on the experience of the operator performing salivary duct cannulation and sialography evaluation; movement artifacts [6,22,35].

When interpreting sialography, it should be remembered that air bubbles, injected together with the contrast medium, may simulate the presence of the calculi [6].

Sialography complications include salivary duct perforations, activation of a dormant inflammation, adverse reactions to iodine contrast medium, bleeding.

Despite all above mentioned facts, sialography, especially in its digital modality, is still regarded as the best diagnostic method for visualisation of a detailed anatomy of the salivary ducts [6,13,22,36]. It allows for visualisation of the main duct, together with its branches, from primary, to quaternary ones [1,6]. Sensitivity of conventional sialography in calculi detection ranges from 64 to 100%, while its specificity from 88 to 100%. Digitalisation of that examination, with the use of subtraction, increased its sensitivity of stone detection up to 96–100%, and its specificity to 88–91.1% [6].

Summing up, sialography requires a lower x-ray radiation dose, as compared to CT. It is more accessible than MRI [36]. Moreover, sialography, owing to its possibilities of a detailed visualisation of anatomical and pathological structures of the salivary ducts, plays an important role in the qualification of patients for sialoendoscopic procedures, and in choosing the strategy of the procedure [13].

Figure 12. Ultrasonogram of the right submandibular gland, salivary stone (7 mm) in the right Wharton's duct (arrow), acoustic shadow behind the calculus (courtesy of Czasopismo Stomatologiczne).

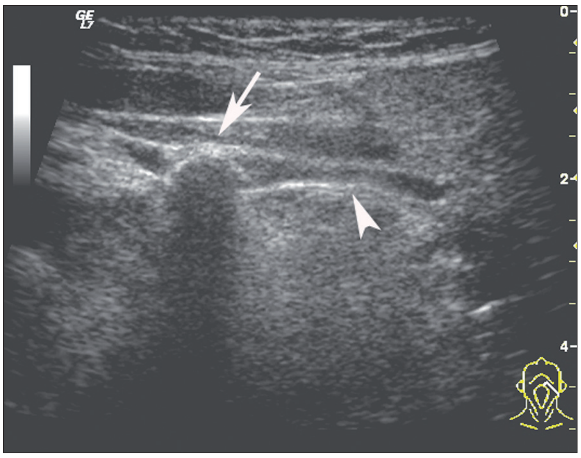

Figure 13. Ultrasonogram of the left submandibular gland, salivary stone (9 mm) in the middle portion of the left Wharton's duct (arrow), acoustic shadow behind the calculus. Dilated proximal segment of left Wharton's duct (arrowhead) (own material).

Ultrasonography

Ultrasonography is regarded by some authors as a method of choice in salivary stone diagnostics. Its sensitivity in calculi detection amounts to 94%, specificity – 100%, and accuracy – 96% [1,5,10]. According to Jäger et al., US sensitivity in sialolithiasis detection is equal to 59.1–93.7%, and its specificity: 86.7–100% [6].

USG is a diagnostic method allowing for non-opaque calculi detection with sensitivity of 80–96% [7,8]. A typical US image of a stone involves: an echogenic, round or oval structure, producing an acoustic shadow (Figure 12) [1,7,9]. Stones in salivary ducts may lead to the distension of the duct above the obstacle, which may be shown on US (Figure 13) [8]. Stones smaller than 2 mm may not produce any acoustic shadow (Figure 14) [1,6–8]. Diagnostic mistakes may concern very small stones in intraparenchymal ducts, with no duct distension [1,7]. Moreover, hyperechogenic air bubbles, mixed with the saliva and simulating stones, may be misleading as well [9].

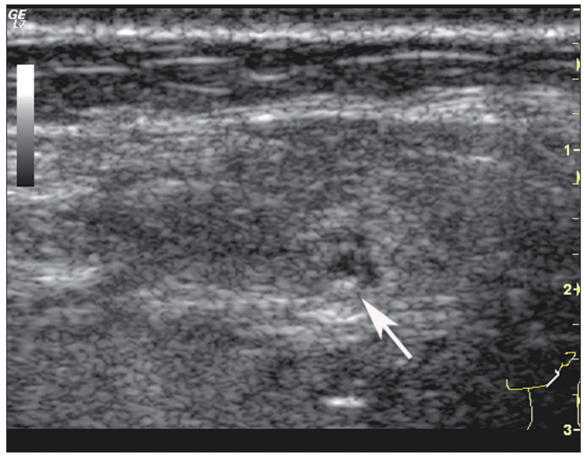

Figure 14. Ultrasonogram of the left submandibular gland, small salivary stone (1.5 mm) in the hilum of the left submandibular gland (arrow) without acoustic shadow (own material).

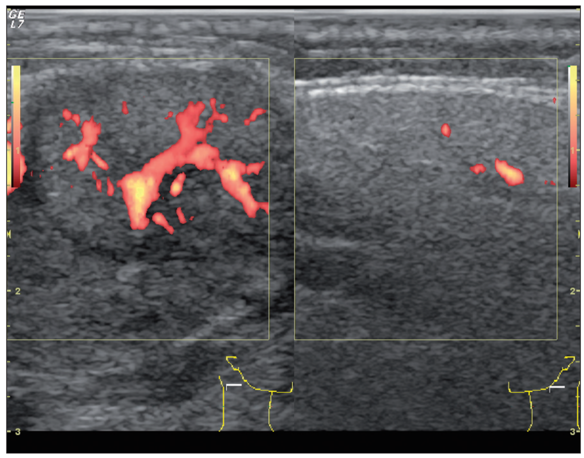

Figure 15. Ultrasonogram of the right and left submandibular glands. The right submandibular gland with the features of inflammatory process – hypoechogenic parenchyma with increased blood flow in Power Doppler. The left submandibular gland normal (own material).

The detection of fine stones may be helped by sialogogue injection, which causes salivary duct dilatation and thus facilitates calculi visualisation [1,7]. Fine stones, in the region of Wharton's duct opening, are hard to visualise, although 65% of cases show salivary duct dilatation [8].

Calculi located close to Wharton's duct opening or in its medial part may be sometimes better visible on US after pressure applied with a finger, from the inside of the oral cavity [9].

In about 50% of the sialolithiasis cases, US images show features of inflammation (Figure 15).

Despite many advantages of this method, US turns out to be less precise in differentiating a cluster of stones from a single, large stone [5].

Computed Tomography

According to some authors, unenhanced CT is the best method in sialolithiasis detection (Figure 16), especially in case of painful salivary glands and suspicion of a few, very tiny calculi [1,5]. A cluster of fine stones is hard to differentiate from one, large stone. That is when CT is recommended [1].

CT detects calcifications with high sensitivity, but its disadvantage is a poor visualisation of salivary ducts and lesions within them, as well as patient's exposition to ionising radiation and a relatively high cost of the examination [2].

The phenomenon of the post-contrast enhancement in CT should be used in suspicion of an abscess that cannot be detected with US.

CT sialography, similarly to the conventional sialography, requires cannulation of the duct opening. Moreover, it exposes patients to a higher dose of radiation, as compared with the conventional sialography. This method allows for simultaneous visualisation of the glandular tissue and the salivary ducts. The salivary glands may be shown in 3D reconstruction. However, CT sialography cannot visualise the secondary and the tertiary branches [6].

Recently, we have witnessed the first, encouraging publications on the use of the volumetric tomography (alternatively called Cone Beam Computed Tomography – CBCT) in sialolithiasis diagnostics [37]. This method produces high-resolution, 3D images of bony structures of the head and neck, with the use of up to 15 times lower ionising radiation dose, and being much cheaper [38,39].

Magnetic Resonance Sialography

Magnetic resonance sialography, as a modality of MRI, was first described in 1996 by Lomas et al. [40]. Being a non-invasive method, it does not require cannulation of the salivary duct opening, and it does not expose patients to ionising radiation or iodine contrast administration. The examination may be carried out in acute inflammation of the salivary gland. This is an alternative of digital subtraction sialography, especially in cases of acute sialoadenitis or failure of salivary opening cannulation [11,22,27,35].

MRI sialography allows for a precise morphological evaluation of the salivary ducts, enabling the visualisation of their tertiary branches [40].

There are different methods of MRI sialography performance. Commonly used are the rapid spin-echo sequences: two- or three-dimensional or single-layer. Capaccio et al. [40] compared the MR sialography with the results of salivary gland US. The examinations were performed before and after stimulation with lemon juice. MR sialography showed secondary branches of the salivary ducts within submandibular salivary glands, and tertiary branches within the parotid glands. MRI confirmed all cases of intraglandular duct dilatation found with USG (Figure 17A,B), additionally, and revealed the coexisting stenoses. MR sialography allowed for visualisation of very tiny stones that could not be found with US [40].

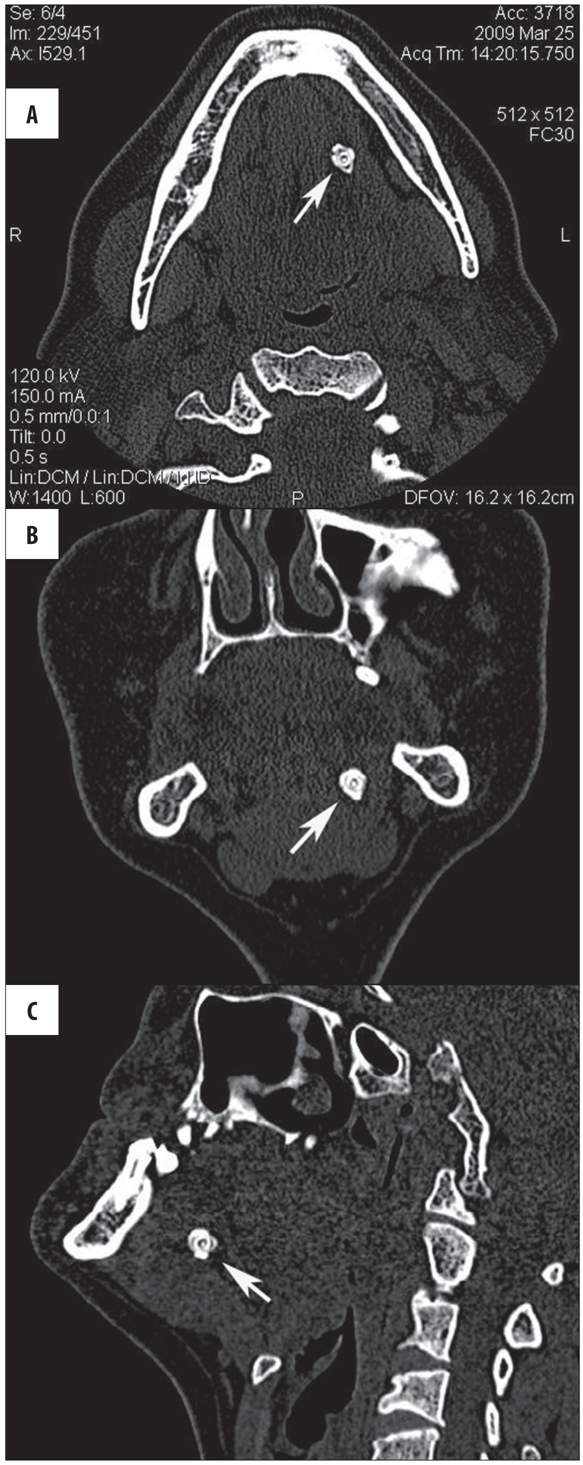

Figure 16. Nonenhanced computed tomography (CT). (**A**) – axial bone CT, large calcified stone (9×7 mm) in the middle segment of the left Wharton's duct (arrow), (**B**) – the same calcified stone (7×6 mm) in coronal view, (**C**) – the same stone (8×7 mm) in sagittal view. The laminar structure of the stone can be seen (own material)

According to Becker et al., MR sialography is a better method for salivary gland evaluation than X-ray sialography or US, as it allows for visualisation of distal salivary ducts. By adding extra MRI sequences for parenchymal imaging, it is

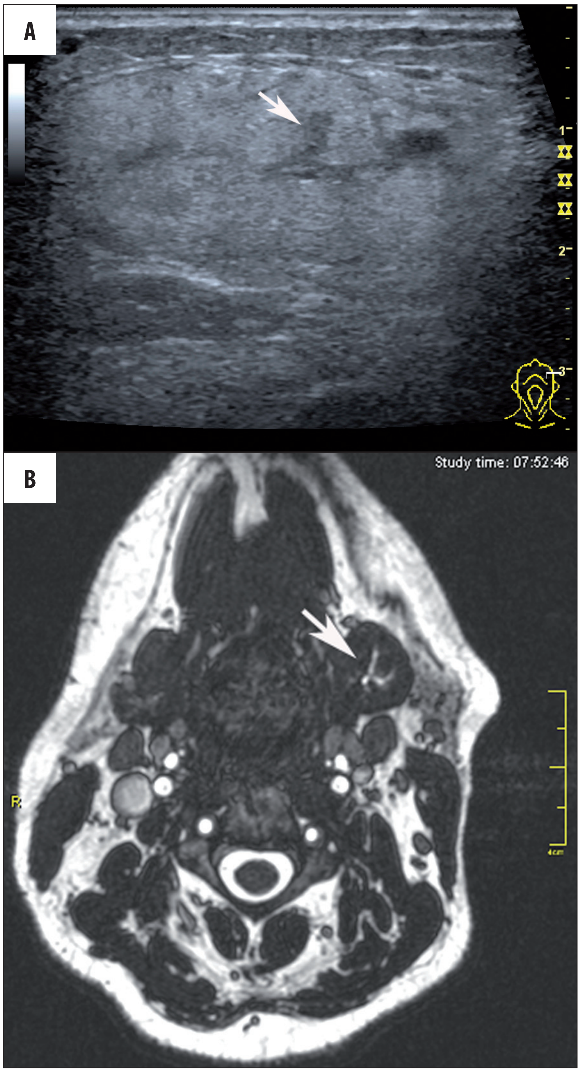

Figure 17. (**A**) Ultrasonogram of the left submandibular gland. The dilated intraglandular salivary ducts can be seen (arrow), (**B**) MRI sialography of the left submandibular gland, 3D CISS sequence; hyperintense dilated intraglandular salivary ducts can be seen (arrow) (own material).

possible to detect some lesions located outside the system of the salivary ducts (e.g. Warthin's tumour) [4].

Becker et al. [36] evaluated MR sialography precision in the detection of calculi and salivary duct stenoses. They used the conventional sialography, US, and sialoendoscopy, as comparative methods. In calculi detection, MR sialography showed a sensitivity of 91%, a specificity of 94–97%, a positive predictive value of 93–97%, and a negative predictive value of 91%. False negative results were obtained in calculi measuring 2–3 mm, located in undilated salivary ducts. Ductal stenosis was evaluated with a sensitivity of 100%, a specificity of 93–98%, a positive predictive value of 87–95%, and a negative predictive value of 100%. Fine stones would be better visualised with initial images, as the MIP reconstructions may omit them due to the hyperintense saliva surrounding the calculi. Salivary duct stenoses would be best visualised with MIP reconstructions (Figure 18). It was found out that MR sialography allows

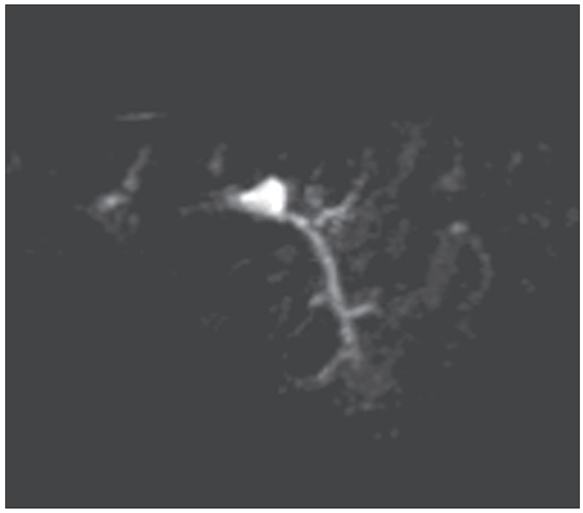

Figure 18. MR sialography of the left submandibular gland, MIP 3D reconstruction. The system of intraglandular salivary ducts and dilated, proximal segment of the left Wharton's duct (courtesy of Czasopismo Stomatologiczne).

for a reliable visualisation of salivary stones and salivary duct stenoses. However, in this work, MR sialography did not distinguish a stone from a dense mucosal plug. Moreover, the amalgam fillings veiled the tiny calculi and stenoses of the salivary ducts. It was also revealed that the peripheral salivary ducts could be better visualised with the conventional X-ray sialography than with MR sialography. As compared to the conventional sialography, the MRI image of the secondary and tertiary branches was of worse spatial resolution (Figure 7B, Figure 17B, Figure 18).

Although the MRI examination allowed for a precise evaluation of salivary calculi and salivary duct stenoses, the normal image did not exclude the presence of small calculi, of 2–3 mm in size, not leading to salivary duct dilatation. That is why, the patients with chronic symptoms and normal MR sialography results were advised by the authors of this study to undergo the conventional sialography and US [35].

Jäger et al. evaluated the usefulness of different sequences of T2-weighted images (Figure 19A–C) in the detection of sialolithiasis of the submandibular gland, by referring the obtained results to the results of US and digital X-ray sialography. MR sialography was performed with the use of strong T2-weighted 3D CISS sequences and T2-weighted rapid spin-echo (RARE) sequences. Twenty-four patients suspected of sialolithiasis were subjected to the analysis. The same group of patients was then subjected to an additional evaluation of the salivary gland parenchyma, with the use of conventional spin-echo T1- and T2-weighted sequences, which required cannulation of the gland opening and administration of gadolinium derivative. Before the examination, patients received lemon juice, in order to increase the saliva production.

Sensitivity and specificity in submandibular calculi detection amounted to 100% and 80% for MR sialography CISS (Constructive Interference in Steady State), and 80% and 100% for MR sialography RARE (Rapid Acquisition with Relaxation Enhancement). MR RARE, due to a low spatial

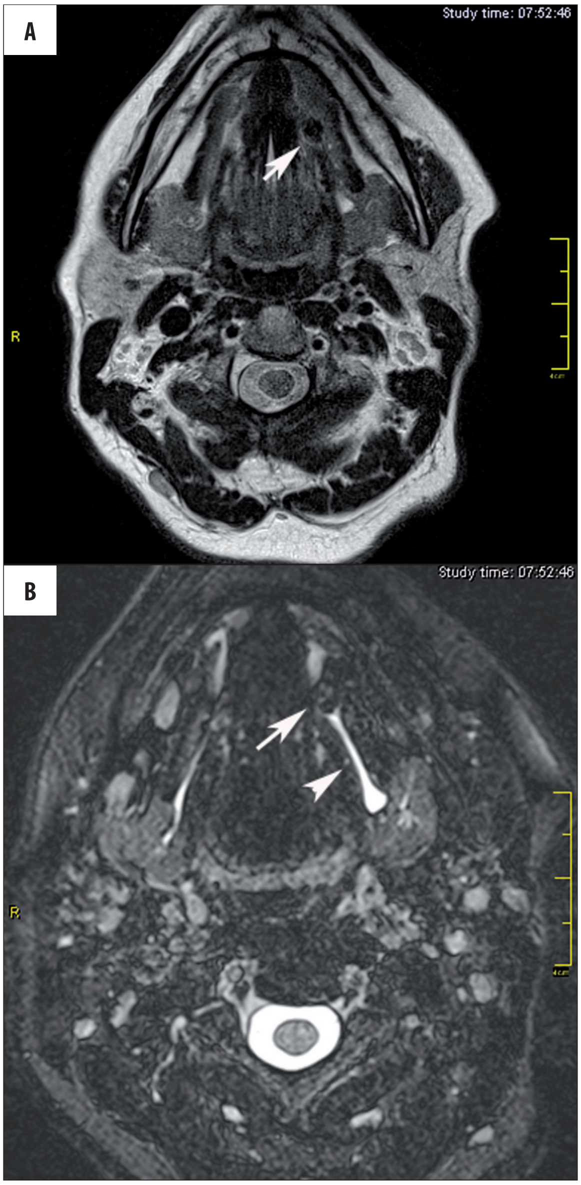

Figure 19. MR sialography of the left submandibular gland, different T2-weighted images sequences, (**A**) – T2WI turbo spin-echo sequence, hypointense calculus in the midddle segment of the left Wharton's duct (arrow), (**B**) – T2WI turbo spin-echo 3D sequence, hypointense calculus in the midddle segment of the left Wharton's duct (arrow), hyperintense dilated proximal segment of the left Wharton's duct (arrowhead), (**C**) – T2WI 3D CISS sequence – hypointense calculus in the midddle segment of the left Wharton's duct (arrow), hyperintense dilated proximal segment of the left Wharton's duct (arrowhead) (courtesy of Czasopismo Stomatologiczne).

resolution, was not able to show fine calculi. Sensitivity and specificity of US amounted to over 80%. Calculi detection in turbo echo-spin T2-weighted images was connected with the sensitivity of 93% and specificity of 100%. In T1-weighted images, the echo-spin sensitivity was evaluated for 47%, and the specificity for 100%. In Wharton's duct visualization, the MR 3D CISS images (followed by T2-weighted and then T1-weighted images) were significantly better from the RARE images. Intraglandular branches of the salivary ducts would be better visualised with RARE images, than with turbo spin-echo images. T2 TSE images were, on the other hand, better than T1 SE in the visualisation of Wharton's duct and its intraglandular branches. In T1-weighted images, the intraglandular primary and secondary branches were not visible at all.

MR sialography images obtained with 3D CISS sequences are characterised by a high resolution and sensitivity in the evaluation of high-signal-intensity, fluid-filled structures. This is a sequence allowing for intraglandular visualisation of the salivary duct system, with a similar ability (to the one observed in digital sialography) to present the anatomy of salivary ducts. However, in 3D CISS sequences, it is possible to visualise the secondary branches only. The tertiary and quatrinary branches, due to their small diameter (0.4 and 0.2 mm) may be visualised with digital sialography only. An important disadvantage of MR sialography 3D CISS is a long acquisition time and susceptibility to movement artifacts [6].

In one of their papers, Kalinowski et al. [22] compared the diagnostic efficacy of two imaging methods in calculi detection. These were MR sialography, T2 TSE, performed with a single-shot technique, and digital subtraction sialography. The sensitivity and specificity of MR sialography in sialolithiasis detection amounted to 80% and 98% (respectively). With conventional sialography, this was 90% and 98%. The sensitivity and specificity in parotid gland lithiasis diagnosis amounted to 100% and 98% (respectively) for both sialography and MR sialography. Sensitivity of submandibular lithiasis detection was equal to 86% for conventional X-ray sialography and 71% for MR sialography.

In MR sialography, the diagnosis is based nearly exclusively on indirect symptoms, such as the images of full ductal obstruction with signal loss and prestenotic dilatation. That is why fine stones that do not lead to salivary duct occlusions may remain undetected. This concerns primarily

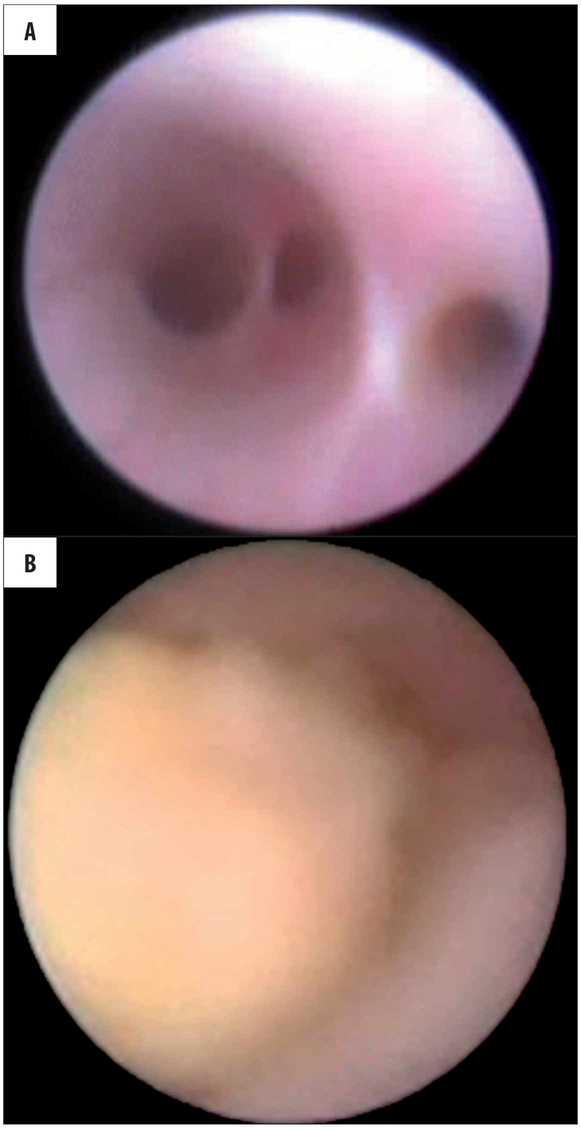

such calculi that are located close to the openings of the ducts or are placed in narrow, intraglandular ducts. MR sialography limitation is also connected with its lower spatial resolution unabling the differentiation of partial and of complete occlusions of the salivary ducts [22]. Summing up, MR sialography is considered as a highly effective, non-invasive diagnostic method of visualisation of salivary ducts of large salivary glands, especially in cases of acute sialoadenitis.

Sialoendoscopy

The causes of salivary duct stenosis remain unknown in 5–10% of cases. The diagnostic gap is filled by sialoendoscopy that allows for a direct visualisation of the salivary duct lumen, i.e. visualisation of calculi (Figure 20B), mucosal plugs, foreign bodies and polyps. Endoscopic diagnostically-therapeutic techniques used within the salivary glands were introduced to the clinical practice at the beginning of 1990's. They were used mainly for the treatment of the inflammatory conditions of the salivary glands and obstructions of the salivary ducts [13].

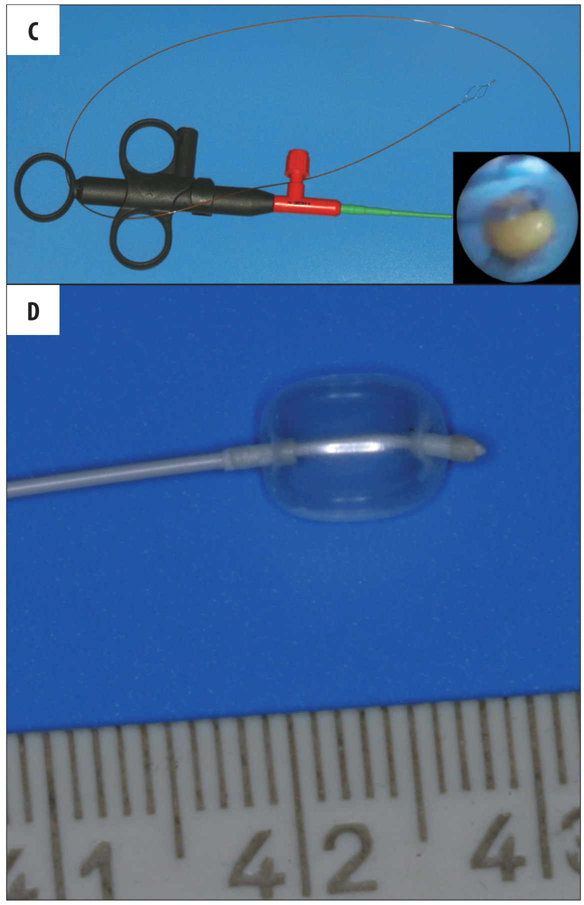

Figure 20. Sialoendoscopy. (**A**) – sialoendoscopic view of intraglandular branches of Stensen's duct, (**B**) – sialoendoscopic view of the calculus inside the Wharton's duct, (**C**) – Dormia basket, in the left lower corner the retrieved calculus, (**D**) – baloon-tipped catheter (own material).

Sialoendoscopy enabled the surgeons to examine the salivary ducts from the inside (Figure 20A). Combination of sialoendoscopy with therapeutic procedures increases the frequency of sialography [13]. X-ray examinations are then used to qualify a patient for a surgical procedure.

Some authors recommend dilatation of the ductal openings before performing sialoendoscopy. Others recommend papillotomy [13]. During sialoendoscopy, the operators use very small tools and a camcorder, to reach the proximal parts of the salivary ducts. Sialoendoscopy includes performance of the following procedures: calculi removal with the use of the Dormia basket (Figure 20C), dilatation of the stenosed salivary ducts with the use of balloons (Figure 20D), as well as stenosis correction [14]. At the end of the sialoendoscopic procedure, a stent, 2–3 cm long, is left in the salivary duct for 7–10 days. The retained stent facilitates the healing process and the salivary drainage.

Moreover, with the use of sialoendoscopy, it is possible to diagnose salivary duct inflammation [15].

New therapeutic modalities use extracorporeal or intracorporeal crushing of the salivary gland calculi. The crushed stones can be flushed out with saliva, through natural salivary duct openings [2].

Experimental Research

In one of their experimental research articles, Shimizu et al. [3] combined the use of sialography with ultrasonography. Different contrast agents were injected into narrow catheters: saline, Urographine in concentration of 76%, Lipidol Ultra-Fluid in concentration of 67, 90, and 100%, barium sulphate in concentration of 1 and 5%, as well as Levovist 200 mg/ml. The injection rate ranged from 0.001 ml/sec to 0.1 ml/sec. The authors were trying to find the interrelation between Doppler signal intensity and the type, concentration and injection rate of the administered substances.

Levovist, Lipiodol Ultra-Fluid in concentrations of 67% and 90%, as well as barium sulphate solutions produced a Doppler signal. Among all substances, the highest Doppler signal intensity was obtained with Levovist. The signal recorded with Lipidol was less intensive, and the mixture of Lipidol and saline produced a high-intensity signal, irrespective of their concentration. Doppler signal was received at every infusion rate, but the researchers revealed a proportionate dependence between signal intensity and the injection rate of all signal-producing fluids. Thus, the revealed interrelations create potential possibilities of US sialography application in clinical practice [30].

Conclusions

Conventional X-ray sialography, and especially the digital subtraction sialography, combined with ultrasonography, is the method of choice in visualisation of salivary gland calculi. Sialography precisely show the subtle morphology of salivary ducts, e.g. stenoses, and in case of calculi presence – their location and number. Digital subtraction sialography, apart from its enormous diagnostic potential, can also be used as a therapeutic method. Interventional sialography is less invasive than the surgical treatment. Moreover, sialography and US are inevitable in patient's qualification for diagnostic and therapeutic sialoendoscopy, owing to which it is now possible to avoid sialoadenectomy. An alternative, non-invasive diagnostic method of salivary gland calculi and salivary duct stenosis detection is MRI or MR sialography. These methods do not require cannulation of the salivary duct openings, nor the administration of the contrast medium. It does not expose patients to ionising radiation either. The MR sialography may be carried out in acute sialoadenitis.

As the last resort, in search for very fine and multiple calculi, it is possible to apply the unenhanced computed tomography of the salivary glands.

References:

1. Madani G, Beale T: Inflammatory Conditions of the Salivary Glands. Semin Ultrasound CT MRI, 2006; 27(6): 440–51
2. Drage NA, Brown JE, Escudler MP et al: Interventional radiology in the removal of salivary calculi. Radiology, 2000; 214(1): 139–42
3. Langlais RP: Diagnostic imaging of the jaws. Williams and Wilkins, 1995; 623–27
4. Rabinov JD: Imaging of salivary gland pathology. Radiol Clin North Am, 2000; 38(5): 1047–57
5. Yousem DM, Kraut MA, Chalian AA: Major Salivary Gland Imaging. Radiology, 2000; 216(1): 19–29
6. Jäger L, Menauer F, Holzknecht N et al: Sialolithiasis: MR Sialography of the Submandibular Duct – An Alternative to Conventional Sialography and US? Radiology, 2000; 216(3): 665–71
7. Koischwitz D, Gritzmann N: Ultrasound of the neck. Radiol Clin North Am, 2000; 38(5): 1029–45
8. Alyas F, Lewis K, Williams M et al: Diseases of the submandibular gland as demonstrating using high resolution ultrasound. Br J Radiol, 2005; 78(928): 362–69
9. Białek EJ, Jakubowski W, Zajkowski P et al: US of the major salivary glands: anatomy and spatial relationships, pathologic conditions, and pitfalls. Radiographics, 2006; 26(3): 745–63
10. Wong KT, Ahuja AT, Yuen HY et al: Ultrasound of salivary glands. ASUM Ultrasound Bulletin, 2003; 6(3): 18–22
11. Obaid H, Sinha R, Robinson L: Submandibular sialogram performed through a Wharton's duct fistula: Technical adaptation of conventional technique. Eur J Radiol, 2006; 60(1): 56–57
12. Buckenham TM, George CD, McVicar D et al: Digital sialography: imaging and intervention. Br J Radiol, 1994; 67(798): 524–29
13. Hasson O: Sialoendoscopy and Sialography: Strategies for Assessment and Treatment of Salivary Gland Obstructions. J Oral Maxillofac Surg, 2007; 65(2): 300–4
14. Nahlieli O, Shacham R, Yoffe B et al: Diagnosis and treatment of strictures and kinks in salivary gland ducts. J Oral Maxillofac Surg, 2001; 59: 484–90
15. Yuasa K, Nakhayama E, Ban S et al: Submandibular gland duct endoscopy. Diagnostic value for salivary duct disorders in comparison to conventional radiography, sialography, and ultrasonography. Oral Surg Oral Med Oral Pathol Oral Radiol Endod, 1997; 84(5): 578–81
16. Yu C, Zheng L, Yang C et al: Causes of chronic obstructive parotitis and management by sialoendoscopy. Oral Surg Oral Med Oral Pathol Oral Radiol Endod, 2008; 105(3): 365–70
17. White SC, Pharoah MJ: Radiologia Stomatologiczna. Wydawnictwo Czelej, Wyd. I 2002: 621–28
18. Forman WH: Subtraction sialography. Radiology, 1977; 122(2): 533
19. Kalk WW, Vissink A, Fred KL et al: Morbidity from parotid sialography. Oral Surg Oral Med Oral Pathol Oral Radiol Endod, 2001; 92(5): 572–75
20. Eracleous E, Kallis S, Tziakouri C et al: Sonography, CT, CT sialography, MRI and MRI sialography in investigation of the facial nerve and the differentiation between deep and superficial parotid lesions. Neuroradiology, 1997; 39(7): 506–11
21. Szolar DH, Groell R, Braun H et al: Ultrafast Computed Tomography and three-dimensional image processin of CT sialography in patients with parotid masses poorly defined by magnetic resonance imaging. Acta Otolaryngol, 1996; 116(1): 112–18
22. Kalinowski M, Heverhagen JT, Rehberg E et al: Comparative Study of MR Sialography and Digital Subtraction Sialography for Benign Salivary Gland Disorders. AJNR Am J Neuroradiol, 2002; 23(9): 1485–92
23. Eyjólfsson O, Nordshus T, Dahl T: Sialography and CT-sialography in the diagnosis of parotid masses. Acta Radiol Diagn (Stockh), 1984; 25(5): 361–64
24. Bryan RN, Miller RH, Ferreyro RI et al: Computed tomography of the major salivary glands. AJR Am J Roentgenol, 1982; 139(3): 547–54
25. Nixon PP, Lancer J, Bradley MJ: Case Report: Percutaneous Sialography. Clin Radiol, 1998; 53(5): 381–83
26. Kalk WW, Vissink A, Spijkervet FK et al: Parotid sialography for diagnosing Sjögren syndrome. Oral Surg Oral Med Oral Pathol Oral Radiol Endod, 2002; 94(1): 131–37

27. McGahan JP, Walter JP, Bernstein L: Evaluation of the Parotid Gland. Comparison of Sialography, Non-contrast Computed Tomography and CT Sialography. Radiology, 1984; 152(2): 453–58
28. Rabinov K: Improved instruments for sialography. Radiology, 1981; 141(1): 245–46
29. Carroll BA, Goldin AR: Sialography: A simplified technique. Radiology, 1975; 117(1): 220–21
30. Shimizu M, Tokumori K, Okamura K et al: Possibility of sialographic sonography: A Doppler phantom study. Oral Surg Oral Med Oral Pathol Oral Radiol Endod, 2001; 91(6): 719–27
31. Som PM, Shugar JMA, Train JS et al: Manifestations of Parotid Gland Enlargement: Radiographic, Pathologic, and Clinical Correlations. Part I: The Autoimmune Pseudosialectasias. Radiology, 1981; 141(2): 415–19
32. Ballinger PW: Merrill's atlas of radiographic positions and radiologic procedures; 8th edition; Mosby 1995; 4–10
33. Sutton D, Young JWR: A short textbook of clinical imaging; Springer Verlag 1990; 508
34. Yoshino N, Hosokawa A, Sasaki T et al: Interventional radiology for the non-surgical removal of sialoliths. Dentomaxillofac Radiol, 1996; 25(5): 242–46
35. Becker M, Marchal F, Becker CD et al: Sialolithiasis and Salivary Ductal Stenosis: Diagnostic Accuracy of MR Sialography with a Three-dimensional Extended-Phase Conjugate- Symmetry Rapid Spin- Echo Sequence. Radiology, 2000; 217(2): 347–58
36. Drage NA, Brown JE, Wilson RF: Pain and swelling after sialography: Is it a significant problem? Oral Surg Oral Med Oral Pathol Oral Radiol Endod, 2000; 90(3): 385–88
37. Drage NA, Brown JE: Cone beam computed sialography of sialoliths. Dentomaxillofac Radiol, 2009; 38(5): 301–5
38. Ludlow JB, Ivanovic M: Comparative dosimetry of dental CBCT devices and 64-slice CT for oral and maxillofacial radiology. Oral Surg Oral Med Oral Pathol Oral Radiol Endod, 2008; 106(1): 106–14
39. Scarfe WC, Farman AG, Sukovic P: Clinical applications of cone-beam computed tomography in dental practice. J Can Dent Assoc, 2006; 72(1): 75–80
40. Capaccio P, Cuccarini V, Ottaviani F et al: Comperative Ultrasonographic, Magnetic Resonance Sialographic, and Videoendoscopic Assessment of Salivary Duct Disorders. Ann Otol Rhinol Laryngol, 2008; 117(4): 245–52